Proximity Effects Induced in Graphene by Magnetic Insulators: First-Principles Calculations on Spin Filtering and Exchange-Splitting Gaps

H. X. Yang,[1] A. Hallal,[1] D. Terrade,[1] X. Waintal,[2] S. Roche,[3,4] and M. Chshiev[1]
[1]SPINTEC, CEA/CNRS/UJF-Grenoble 1/Grenoble-INP, INAC, 38054 Grenoble, France
[2]SPSMS-INAC-CEA, 17 rue des Martyrs, 38054 Grenoble, France
[3]CIN2 (ICN-CSIC) and Universitat Autónoma de Barcelona, Catalan Institute of Nanotechnology, Campus UAB, 08193 Bellaterra, Spain
[4]Institucio Catalana de Recerca i Estudis Avançats (ICREA), 08010 Barcelona, Spain
(Received 26 September 2012; published 24 January 2013)

We report on first-principles calculations of spin-dependent properties in graphene induced by its interaction with a nearby magnetic insulator (europium oxide, EuO). The magnetic proximity effect results in spin polarization of graphene π orbitals by up to 24%, together with a large exchange-splitting band gap of about 36 meV. The position of the Dirac cone is further shown to depend strongly on the graphene-EuO interlayer. These findings point toward the possible engineering of spin gating by the proximity effect at a relatively high temperature, which stands as a hallmark for future all-spin information processing technologies.

DOI: 10.1103/PhysRevLett.110.046603 PACS numbers: 72.25.−b, 68.65.Pq, 75.70.Ak, 75.70.Cn

Heat dissipation has become the bottleneck for further downsizing complementary metal–oxide–semiconductor devices, and one of the proposed alternatives is to switch the spin without producing charge currents. In practice, the fabrication of components able to simultaneously inject, manipulate, and read out currents based on electron spin stands as an overwhelming material and technological challenge. The combination of semiconductors with magnetic materials remains to date unsuccessful owing to material structural and chemical mismatches [1–4].

Two-dimensional graphene has demonstrated outstanding physical properties such as exceptional electrical, thermal, and mechanical properties [5,6], but also very long spin diffusion lengths up to room temperature [7–13]. This offers an unprecedented platform for the advent of lateral spintronics in which a complete integration of spin injection, manipulation, and detection could lead to ultrafast electronic circuits compatible with more-than-Moore complementary metal–oxide–semiconductor and nonvolatile low energy magnetoresistive random-access memory devices [14]. However, a fundamental challenge lies in the development of external ways to control (gate) the propagation of spin (polarized) currents at room temperature, in view of designing spin logics devices [15,16].

Spin in graphene can be influenced by the presence of local magnetic ordering intentionally generated by material design or defects. For instance, edge magnetism has been shown to develop in graphene nanoribbons (a few nanometers wide) for certain edge geometries [17,18], or the hole structure of graphene nanomesh [19] was also theoretically proposed to offer robust and room temperature magnetic states able to affect spin transport [20]. A lot of interest is also currently devoted to the tunability of spin-polarized currents and magnetoresistance signals by intentional defects, or depositing atoms or molecules (such as hydrogen [21,22] or 3d and 5d metal atoms [23–27] or large molecules [28]). Finally, the growth of graphene on magnetic metallic substrates was also proposed as a route for tailoring graphene spin properties [29–33]. However, magnetic conducting substrates, which naturally short-circuit the graphene layer, fundamentally restrict the design of novel types of spin switches. Therefore, much effort has been diverted to the use of magnetic insulators to induce magnetism in graphene by the proximity effect [34–38].

In this Letter, we report tunable magnetic proximity effects induced on graphene by a nearby magnetic insulator. We focus on europium oxide (EuO), which has recently been successfully grown experimentally on graphene [39]. By using *ab initio* simulations, with both VASP and SIESTA codes, the structure and spin-dependent electronic properties of graphene-EuO junctions are computed. Our findings show that the magnetic interaction induces a large spin polarization of graphene π orbitals, leading to about 24% together with a large exchange-splitting band gap of 36 meV.

The Vienna *ab initio* simulation package (VASP) [40–42] is used for structure optimization, where the electron-core interactions are described by the projector augmented wave method for the pseudopotentials [43], and the exchange correlation energy is calculated within the generalized gradient approximation of the Perdew-Burke-Ernzerhof form [44,45]. The cutoff energies for the plane wave basis set used to expand the Kohn-Sham orbitals are 520 eV for all calculations. A $4 \times 4 \times 1$ k-point mesh within Monkhorst-Pack scheme is used for the Brillouin zone integration. Structural relaxations and total energy calculations are performed ensuring that the Hellmann-Feynman forces acting on ions are less than 10^{-3} eV/Å. Because Eu is a heavy

element with atomic number 63 and its outer shell ($4f^7 6s^2$) contains $4f$ electrons, the generalized gradient approximation (GGA) approach fails to describe the strongly correlated localized $4f$ electrons of EuO and predicts a metallic ground state of EuO, whereas a clear band gap is observed in experiments [46,47]. Thus, we introduce a Hubbard-U parameter to describe the strong intra-atomic interaction in a screened Hartree-Fock-like manner. For the parameter choice, we fix the on-site Coulomb repulsion and exchange interaction on an Eu $4f$ orbital as 8.3 and 0.77 eV, respectively. For oxygen $2p$ orbitals, the on-site Coulomb and exchange parameters are 4.6 and 1.2 eV, respectively [46].

Using the GGA + U method, the structure is first optimized from energy considerations and the obtained value of a 5.188 Å lattice constant is found to be very close to experimental data (5.141 Å) with an error of only 0.9% and close to the LDA + U method (5.158 Å). With the optimized lattice, we calculated the density of states for EuO with a ferromagnetic state, where a band gap is observed with a value of about 1.0 eV. This is consistent with the experimental optical absorption gaps of 0.9 and 1.2 eV observed below and above the magnetic transition temperature [48,49]. Here the GGA + U method gives better results than the LDA + U. The LDA + U method gives a 0.7 eV band gap with a ferromagnetic spin arrangement, and 1.2 or 1.3 eV for 111 antiferromagnetic spin configuration (AFMI) or the NiO-type antiferromagnetic spin configuration (AFMII), respectively.

We next consider the lattice mismatch between graphene and EuO. If we use experimental values, the graphene lattice constant is 2.46 Å, and the EuO one is 5.141 Å. On a EuO (111) substrate, a 2×2 surface unit cell is about 7.2704 Å, which can fit with a 3×3 unit cell of graphene with a lattice mismatch of about 1.46%. If the GGA + U optimized lattice constant is used, 5.188 Å, the mismatch is much smaller (less than 1%). In our calculations, we used the theoretical lattice constant.

With such a reasonable lattice matching, we first evaluated the stability of graphene on a EuO surface before studying spintronic properties. Two structures with graphene on an oxygen terminated surface and on Eu terminated surfaces of EuO are considered. For these two configurations, we have the same number of atoms: 18 carbon atoms, 24 oxygen, and 24 europium. The calculated total energies are found to be −544.50389 and −545.16824 eV for graphene on O-terminated and Eu-terminated EuO surfaces, respectively. One can see that with the Eu-terminated surface, the system is more stable with an energy gain of 0.67 eV. Thus, we use the lowest energy configuration of 12 layers of EuO as a substrate. To avoid the bottom surface effects on graphene, the bottom oxygen atoms are terminated by hydrogen to simulate graphene on a semi-infinite EuO surface. For all calculations, the vacuum length is chosen larger than 20 Å. The optimized distance between the EuO substrate and the graphene is shown in Fig. 1 with a vertical distance of around 2.57 Å (nearest C-Eu distance of 2.77 Å).

Using the SIESTA package [50] and the optimized structure of graphene on EuO shown in Figs. 1(a) and 1(b), we calculate the local density of states for this system [Figs. 2(c)–2(h)] with LDA + U for the exchange correlation functional. The self-consistent calculations are performed with an energy cutoff of 600 Ry and with a $4 \times 4 \times 1$ k-point grid. A linear combination of numerical atomic orbitals with a double-ζ polarized basis set is used. Due to the existence of the EuO substrate, the two sublattices of freestanding graphene break into six folders as shown in Fig. 2(a) with different colors and letters. In this structure, the calculated magnetic moment of surface Eu atoms is found to be a little bit enhanced, about $7.1\mu_B$, compared to the bulk value of $6.9\mu_B$. Additionally, the sublayer oxygen atoms are found to be spin polarized as well, with a magnetic moment of about $-0.03\mu_B$. The interaction with the magnetic substrate remarkably affects the magnetic properties of graphene. As shown in Fig. 2(b), the average spin polarization in the graphene layer is found to be about 24%. Here, spin polarization is defined as a difference between minority and majority states normalized by the total density of states at the Fermi level, i.e., $p = (n^{\downarrow} - n^{\uparrow})/(n^{\downarrow} + n^{\uparrow})$.

Because these 18 carbon atoms are broken into 6 symmetry groups, the contribution of each to the total spin polarization is different. The spin polarization of magenta

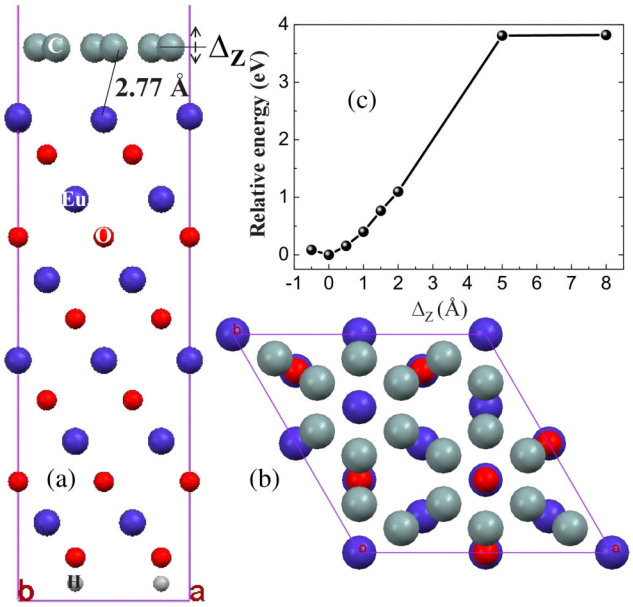

FIG. 1 (color online). (a) side view and (b) top view of the calculated crystalline structures for graphene on top of a six bilayer EuO film. The bottom of EuO is terminated with hydrogen atoms. (c) relative energy (to the optimized structure) of graphene-EuO as a function of shifting distance (Δ_Z) between the graphene and the substrate.

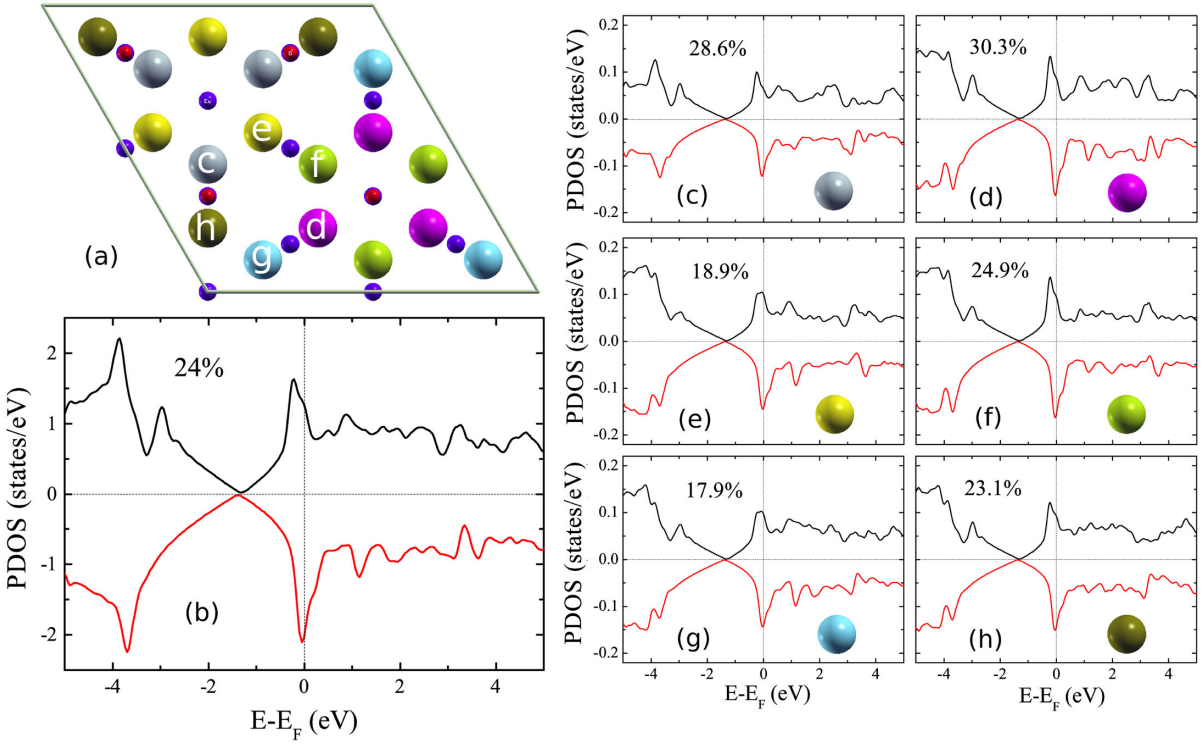

FIG. 2 (color online). (a) The six sublattices of graphene on EuO represented with different colors and letters. (b) Total density of states of p_z orbitals of graphene. (c), (d), (e), (f), (g), (h) Local density of states on each inequivalent atom of the supercell shown in (a). The spin polarizations in (b) to (h) are calculated by comparing the density of states between minority and majority states normalized by the total density of states at Fermi level, i.e., $p = (n^{\downarrow} - n^{\uparrow})/(n^{\downarrow} + n^{\uparrow})$.

(d) atoms can reach up to 30.3% [Fig. 2(d)], while for the yellow (e) and blue (g) ones, spin polarization is about 18% [Figs. 2(e) and 2(g)]. As shown in Fig. 2(b), the spin polarization is induced on the p_z orbital, namely on the π bond.

We now scrutinize the proximity effect on the graphene band structures. In freestanding graphene, the honeycomb structure can be seen as a triangular lattice with a basis of two atoms per unit cell, with 2D lattice vectors $\mathbf{A}_0 = \frac{a_0}{2}(\sqrt{3}, 1)$ and $\mathbf{B}_0 = \frac{a_0}{2}(\sqrt{3}, -1)$, where a_0 is the graphene lattice. Of particular importance for the physics of graphene are the two $\mathbf{K}$ and $\mathbf{K}'$ points at the inequivalent corners of the graphene Brillouin zone $\mathbf{K} = \frac{2\pi}{a_0}(\frac{1}{\sqrt{3}}, \frac{1}{3})$ and $\mathbf{K}' = \frac{2\pi}{a_0}(\frac{1}{\sqrt{3}}, -\frac{1}{3})$, which are called Dirac points. The band dispersion close to the $\mathbf{K}$ (or $\mathbf{K}'$) vector, as $\mathbf{k} = \mathbf{K} + \mathbf{q}$, with $|\mathbf{q}| \ll |\mathbf{K}|$, has the form [51],

$$E_{\pm}(\mathbf{q}) \approx \pm v_F|\mathbf{q}| + O[(q/K)^2], \tag{1}$$

where $\mathbf{q}$ is the momentum measured relative to the Dirac point and v_F is the Fermi velocity, given by $v_F = \sqrt{3}ta_0/2$, with a value $v_F \simeq 1 \times 10^6$ m/s, and t is the nearest-neighbor hopping energy of 2.8 eV.

In the usual case with $\epsilon(\mathbf{q}) = q^2/(2m)$, where m is the electron mass, the velocity, $v = k/m = \sqrt{2E/m}$, changes with energy. In Eq. (1), the Fermi velocity does not depend on the energy or momentum [5].

In the case of graphene on the magnetic insulator EuO, as discussed earlier, the two sublattices have been broken into six groups [Fig. 2(a)] and there is a spin injection to graphene from the EuO substrate. The linear dispersion of the graphene band structure is modified (Fig. 3), with a band gap opening at the Dirac point. More interestingly, this degeneracy lifting at the Dirac point is spin dependent: we have fitted the band structure with a simple spin-dependent Dirac dispersion relation in the presence of a spin-dependent mass (gap) term

$$E_{\sigma}(q) = \pm\sqrt{(\hbar v_{\sigma} q)^2 + (\Delta_{\sigma}/2)^2} \tag{2}$$

and obtain gap widths with values of $\Delta_{\downarrow} = 98$ meV and $\Delta_{\uparrow} = 134$ meV for minority and majority states, respectively, while the Fermi velocities $v_{\downarrow} = 1.40 \times 10^6$ m/s and $v_{\uparrow} = 1.15 \times 10^6$ m/s are also polarized [see inset of Fig. 3]. The corresponding polarization, around 20% for both gaps and velocities, is very significant. There is in particular a large energy window (inside the gap region) where the graphene would be 100% polarized (half-metal) along the majority or minority direction depending on the position of the Fermi level. The observed spin splitting is due to the interaction between C-p_z and Eu-4f states.

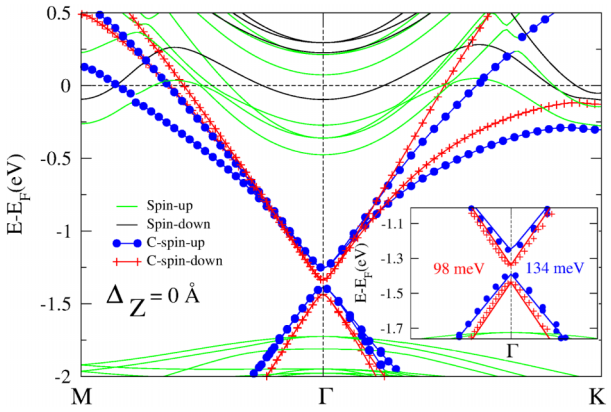

FIG. 3 (color online). Band structure of graphene on EuO. Green (blue) and black (red) represent spin up and spin down bands of EuO (graphene), respectively. Inset: zoom around the Dirac cone, the symbols correspond to DFT data while the lines correspond to the fit according to Eq. (2).

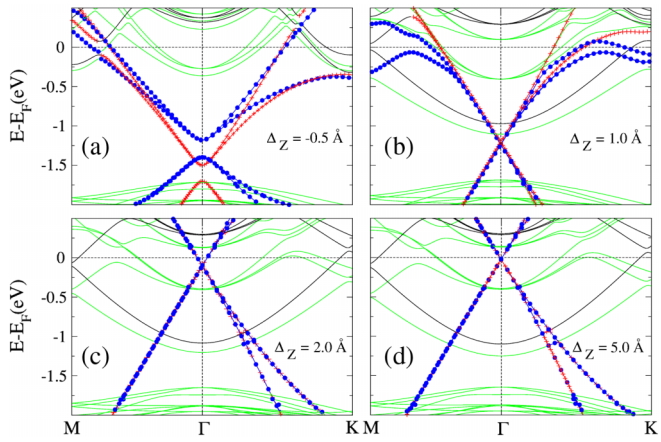

FIG. 4 (color online). Band structures for graphene on EuO with graphene shifted (a) inward (compared to optimized structure) 0.5 Å, (b) outward 1.0 Å, (c) outward 2.0 Å, and (d) outward 5.0 Å, respectively.

Indeed, there is a strong peak of polarized Eu-4f state right below the Fermi level. These polarized states get hybridized with graphene, hence the induced magnetism. This can also be seen from the band structure, where the graphene bands start overlapping with the majority Eu-4f bands.

Because the interaction between graphene and the substrate is quite weak (as evidenced by the large equilibrium distance of 2.57 Å between the graphene and EuO layers), it can be further easily affected by the external environment. To mimic the situation of internal pressure and strain, we calculated the electronic properties for varying the interlayer spacing (Δ_Z) as described in Figs. 1(a) and 1(c). It is found that by interlayer displacement of less than 1 Å, the total energy of the bilayer system changes only by 0.085 and 0.156 eV/cell for displacement inward and outward of 0.5 Å, respectively. This weak modification (for the supercell contains 18 carbon atoms) corresponds to fluctuations in energy per carbon atom in the order of few meV.

Even though the energetics stability with interlayer spacing Δ_Z is weakly affected, the impact on the band dispersion of graphene is markedly strong, as seen in Fig. 4. When compressing the bilayer by 0.5 Å, more electrons (and spins) are transferred to the graphene layer due to enhanced overlap between C p_z and Eu 4f orbitals. Accordingly, the Dirac point is moved deeper inside the valence bands compared to the equilibrium situation [cf. Figs. 3 and 4(a)]. In contrast, for larger layer separation, the Dirac cone is clearly seen to be shifted out from the valence band of EuO, approaching the Fermi level of the system [Figs. 4(b) and 4(c)]. Simultaneously, with the shifting of the Dirac point out of the EuO valence band, the gap between spin-up and spin-down bands is continuously reduced. Finally, for $\Delta_Z = 5$ Å, the spin-up and spin-down branches become almost degenerated and the Dirac point crosses the Fermi level, i.e., approaching a typical band structure characteristics of isolated graphene [Fig. 4(d)].

In conclusion, we have reported first-principles simulations showing that the proximity of a magnetic insulator will induce a strong spin polarization of graphene π orbitals. The europium oxide substrate was found to break the bipartite lattice of graphene into six inequivalent sublattices, causing variable spin polarizations on the new graphene sublattices with an average spin polarization of about 24%. Simultaneously, a band gap develops at the Dirac point with a large exchange splitting of more than 30 meV, larger than anticipated [34]. These theoretical findings deserve further experimental demonstration of the spin filtering effect and the spin-dependent gap in graphene-based structures.

We thank A. Fert, L. Magaud, and J. Velev for fruitful discussions. This work was supported by the Chair of Excellence Program of the Nanosciences Foundation in Grenoble, France, by French National Research Agency (ANR) Projects NANOSIM_GRAPHENE and NMGEM, and by the European Union-funded STREP Project CONCEPT-GRAPHENE.

Note added.—After the submission of this paper, we noticed a successful experimental fabrication of EuO on graphene [52].

[1] S. A. Wolf, D. D. Awschalom, R. A. Buhrman, J. M. Daughton, S. von Molnar, M. L. Roukes, A. Y. Chtchelkanova, and D. M. Treger, Science **294**, 1488 (2001).
[2] I. Žutić, J. Fabian, and S. Das Sarma, Rev. Mod. Phys. **76**, 323 (2004).
[3] C. Chappert, A. Fert, and F. Nguyen Van Dau, Nat. Mater. **6**, 813 (2007).
[4] T. Dietl, Nat. Mater. **9**, 965 (2010).

[5] A. H. Castro Neto, F. Guinea, N. M. R. Peres, K. S. Novoselov, and A. K. Geim, Rev. Mod. Phys. **81**, 109 (2009).

[6] A. K. Geim and K. S. Novoselov, Nat. Mater. **6**, 183 (2007).

[7] N. Tombros, C. Jozsa, M. Popinciuc, H. T. Jonkman, and B. J. van Wees, Nature (London) **448**, 571 (2007).

[8] M. Popinciuc, C. Józsa, P. J. Zomer, N. Tombros, A. Veligura, H. T. Jonkman, and B. J. van Wees, Phys. Rev. B **80**, 214427 (2009).

[9] B. Dlubak, P. Seneor, A. Anane, C. Barraud, C. Deranlot, D. Deneuve, B. Servet, R. Mattana, F. Petroff, and A. Fert, Appl. Phys. Lett. **97**, 092502 (2010).

[10] W. Han and R. K. Kawakami, Phys. Rev. Lett. **107**, 047207 (2011).

[11] T.-Y. Yang, J. Balakrishnan, F. Volmer, A. Avsar, M. Jaiswal, J. Samm, S. R. Ali, A. Pachoud, M. Zeng, M. Popinciuc, G. Güntherodt, B. Beschoten, and B. Özyilmaz, Phys. Rev. Lett. **107**, 047206 (2011).

[12] T. Maassen, J. J. van den Berg, N. IJbema, F. Fromm, T. Seyller, R. Yakimova, and B. J. van Wees, Nano Lett. **12**, 1498 (2012).

[13] B. Dlubak, M.-B. Martin, C. Deranlot, B. Servet, and S. Xavier, Nat. Phys. **8**, 557 (2012).

[14] H. Dery, H. Wu, B. Ciftcioglu, M. Huang, Y. Song, R. Kawakami, J. Shi, I. Krivorotov, I. Zutic, and L. J. Sham, IEEE Trans. Electron Devices **59**, 259 (2012).

[15] Y. G. Semenov, K. W. Kim, and J. M. Zavada, Appl. Phys. Lett. **91**, 153105 (2007).

[16] S. Das. Sarma, S. Adam, E. H. Hwang, and E. Rossi, Rev. Mod. Phys. **83**, 407 (2011).

[17] Y.-W. Son, M. L. Cohen, and S. G. Louie, Nature (London) **444**, 347 (2006).

[18] W. Y. Kim and K. S. Kim, Nat. Nanotechnol. **3**, 408 (2008).

[19] J. Bai, X. Zhong, S. Jiang, Y. Huang, and X. Duan, Nat. Nanotechnol. **5**, 190 (2010).

[20] H.-X. Yang, M. Chshiev, D. W. Boukhvalov, X. Waintal, and S. Roche, Phys. Rev. B **84**, 214404 (2011).

[21] D. Soriano, N. Leconte, P. Ordejon, J.-Ch. Charlier, J.-J. Palacios, and S. Roche, Phys. Rev. Lett. **107**, 016602 (2011).

[22] K. M. McCreary, A. G. Swartz, W. Han, J. Fabian, and R. K. Kawakami, Phys. Rev. Lett. **109**, 186604 (2012).

[23] K. T. Chan, J. B. Neaton, and M. L. Cohen, Phys. Rev. B **77**, 235430 (2008).

[24] Z. Qiao, S. A. Yang, W. Feng, W.-K. Tse, J. Ding, Y. Yao, J. Wang, and Q. Niu, Phys. Rev. B **82**, 161414(R) (2010).

[25] J. Ding, Z. Qiao, W. Feng, Y. Yao, and Q. Niu, Phys. Rev. B **84**, 195444 (2011).

[26] H. Zhang, C. Lazo, S. Blugel, S. Heinze, and Y. Mokrousov, Phys. Rev. Lett. **108**, 056802 (2012).

[27] H. Jiang, Z. Qiao, H. Liu, J. Shi, and Q. Niu, Phys. Rev. Lett. **109**, 116803 (2012).

[28] J. Park, S. B. Jo, Y.-J. Yu, Y. Kim, J. W. Yang, W. H. Lee, H. H. Kim, B. H. Hong, P. Kim, K. Cho, and K. S. Kim, Adv. Mater. **24**, 407 (2012); W. Y. Kim and K. S. Kim, Acc. Chem. Res. **43**, 111 (2010); J. W. Yang, G. Lee, J. S. Kim, and K. S. Kim, J. Phys. Chem. Lett. **2**, 2577 (2011).

[29] A. Varykhalov, J. Sanchez-Barriga, A. M. Shikin, C. Biswas, E. Vescovo, A. Rybkin, D. Marchenko, and O. Rader, Phys. Rev. Lett. **101**, 157601 (2008).

[30] M. Weser, Y. Rehder, K. Horn, M. Sicot, M. Fonin, A. B. Preobrajenski, E. N. Voloshina, E. Goering, and Yu. S. Dedkov, Appl. Phys. Lett. **96**, 012504 (2010).

[31] Y. Cho, Y. C. Choi, and K. S. Kim, J. Phys. Chem. C **115**, 6019 (2011).

[32] O. Rader, A. Varykhalov, J. Sanchez-Barriga, D. Marchenko, A. Rybkin, and A. M. Shikin, Phys. Rev. Lett. **102**, 057602 (2009).

[33] G. Giovannetti, P. A. Khomyakov, G. Brocks, V. M. Karpan, J. van den Brink, and P. J. Kelly, Phys. Rev. Lett. **101**, 026803 (2008).

[34] H. Haugen, D. Huertas-Hernando, and A. Brataas, Phys. Rev. B **77**, 115406 (2008).

[35] P. Michetti and P. Recher, Phys. Rev. B **84**, 125438 (2011).

[36] I. Vobornik, U. Manju, J. Fujii, F. Borgatti, P. Torelli, D. Krizmancic, Y. S. Hor, R. J. Cava, and G. Panaccione, Nano Lett. **11**, 4079 (2011).

[37] Z. P. Niu, F. X. Li, B. G. Wang, L. Sheng, and D. Y. Xing, Eur. Phys. J. B **66**, 245 (2008).

[38] D. Liu, Y. Hu, H. Guo, and X. F. Han, Phys. Rev. B **78**, 193307 (2008).

[39] D. F. Forster, T. O. Wehling, S. Schumacher, A. Rosch, and T. Michely, New J. Phys. **14**, 023022 (2012).

[40] G. Kresse and J. Hafner, Phys. Rev. B **47**, 558 (1993).

[41] G. Kresse and J. Furthmuller, Phys. Rev. B **54**, 11169 (1996).

[42] G. Kresse and J. Furthmuller, Comput. Mater. Sci. **6**, 15 (1996).

[43] P. E. Blochl, Phys. Rev. B **50**, 17953 (1994).

[44] Y. Wang and J. P. Perdew, Phys. Rev. B **44**, 13298 (1991).

[45] G. Kresse and D. Joubert, Phys. Rev. B **59**, 1758 (1999).

[46] N. J. C. Ingle and I. S. Elfimov, Phys. Rev. B **77**, 121202 (2008).

[47] A. Mauger and C. Godart, Phys. Rep. **141**, 51 (1986).

[48] J. Schoenes and P. Wachter, Phys. Rev. B **9**, 3097 (1974).

[49] P. V. Lukashev, A. L. Wysocki, J. P. Velev, M. van Schilfgaarde, S. S. Jaswal, K. D. Belashchenko, and E. Y. Tsymbal, Phys. Rev. B **85**, 224414 (2012).

[50] J. M. Soler, E. Artacho, J. D. Gale, A. Garcìa, J. Junquera, P. Ordejón and Daniel Sánchez-Portal, J. Phys. Condens. Matter **14**, 2745 (2002).

[51] P. R. Wallace, Phys. Rev. **71**, 622 (1947).

[52] A. G. Swartz, P. M. Odenthal, Y. Hao, R. S. Ruoff, and R. K. Kawakami, ACS Nano **6**, 10063 (2012).